

## Surface structure and adsorption properties of multiwalled carbon nanotubes

S. Ya. Brichka,\* L. A. Belyakova, G. P. Prikhod'ko, and N. V. Roik

*Institute of Surface Chemistry, National Academy of Sciences of Ukraine,  
17 ul. Generala Naumova, 03164 Kiev, Ukraine.*

*E-mail: serg\_1971@ukr.net*

The pore structure, sorption parameters, and chemical composition of the surface of multiwalled carbon nanotubes synthesized by catalytic pyrolysis were determined. The dependences of the amount of cholic acid adsorbed by the nanotube surface on time, pH, and concentration of an equilibrium solution were studied. Physical adsorption of cholic acid is mainly the outcome of nonspecific interactions between the acid and the surface of the nanotubes.

**Key words:** adsorption, carbon nanotubes, cholic acid.

An increase in the content of cholesterol and products of its metabolism, first of all, bile acids, provokes a series of serious diseases of liver, kidney, and cardiovascular system.<sup>1,2</sup> Currently, to control the content of bile acids in a living organism, enterosorbents, mainly, anion-exchange resins,<sup>3</sup> are used. However, search for new sorbents is being continued because of a low selectivity of the known sequestrant adsorbents and a slow adsorption rate.<sup>4</sup> We have found<sup>5</sup> that, in addition to good kinetic parameters, modified silicas have a higher sorption capacity compared to that of the polymeric adsorbents of medical design (cholestyramine).<sup>5</sup> Since interactions between the hydrophobic segments of bile acids and hydrophobic regions of the adsorbent surface contribute substantially to adsorption, hydrophobization of the surface of highly dispersed silica also increases the amount of bile acids adsorbed.<sup>6</sup> Cholic acid (CHA, C<sub>24</sub>O<sub>5</sub>H<sub>40</sub>) is a primary bile acid, being the main product of cholesterol conversion. From the chemical point of view, this is the most appropriate test molecule for the estimation of the affinity of the adsorbent surface to bile acids, because CHA is intermediate in the series of these acids in terms of acidity (pK<sub>a</sub> 5.0) and hydrophobicity, which can be characterized by the partition constant between octanol and water (log P<sub>o/w</sub> = 3.04–3.36).<sup>1</sup>

Carbon nanotubes (CNTs) have high specific surface (100–1500 m<sup>2</sup> g<sup>-1</sup>) and are considered as a new class of adsorbents.<sup>7</sup> A specific feature of the CNTs is the presence of internal cavities in which molecules can be adsorbed through volume filling.<sup>8</sup> The polymeric nature of the CNTs results in a variety of their chemical structures. A series of experimental data indicates that the cross sections of the CNTs are polygons containing defect regions with a high concentration of the sp<sup>3</sup>-hybridized carbon atoms. Defects in the form of oxygen-containing

functional groups (up to 2 mmol g<sup>-1</sup>) are also formed upon the interaction of the CNTs with air oxygen.<sup>9,10</sup> It is important to reveal the contribution of these defects to the adsorption capacity of the CNTs.

The present work is aimed at studying a relationship between the surface structure and adsorption properties of the multiwalled carbon nanotubes.

### Experimental

Carbon nanotubes were synthesized by a procedure described in detail previously.<sup>11</sup> At the first stage, a heterogeneous oxide catalyst with the composition FeAlMo<sub>0.07</sub> was prepared from the corresponding salts. A gas mixture of argon and reactants (ethylene : hydrogen = 2 : 1) was introduced to a reactor containing the catalyst and rotated with a rate of 60–90 rpm. The mixture was heated to 680 °C. As a result of the reduction of iron and molybdenum and ethylene pyrolysis, CNTs were formed. To purify them from the catalyst and other carbon phases, the CNT samples were treated with concentrated HNO<sub>3</sub> for 12 h at 80 °C and calcined for 0.5 h at 650 °C in air. The weight loss of the carbon material was more than 60%, and the amount of amorphous carbon decreased, according to electron microscopic data, to 5–10%.

The prepared CNTs were identified using a JEM-100CXII transmission electron microscope. The carbon nanotubes were studied by X-ray photoelectron spectroscopy on an XPS SERIES-800 Kratos Analytical instrument using monochromatic Al-K $\alpha$  radiation with an energy of 1486.6 eV. IR spectra of the CNTs and cholic acid were recorded on a Thermo Nicolet NEXUS FT-IR instrument in the range 4200–400 cm<sup>-1</sup>. Complete thermal analysis was carried out on a Q-1500 D derivatograph in a temperature range of 20–1000 °C with a heating rate of 10 °C min<sup>-1</sup> in air. The structural and adsorption characteristics of the synthesized CNTs were calculated from isotherms of low-temperature nitrogen adsorption–desorption measured on a Kelvin 1042 unit (Costech Microanalytical). Samples of the

CNTs were preliminarily degassed in a helium flow for 7 h at 110 °C to prevent thermal destruction of CHA. The specific surface was calculated by the Brunauer—Emmett—Teller (BET) method,<sup>12</sup> and the pore size distribution was determined using an earlier described method.<sup>13</sup>

Adsorption of cholic acid (Fluka, purity  $\geq 99.5\%$ ) was studied by the method of individual weighed samples at 20 °C. To determine the time needed to achieve adsorption equilibrium, weighed samples of the CNTs (0.05 g) were brought in contact with a  $1 \cdot 10^{-4}$  M aqueous solution of cholic acid and stored for 0.5–72 h with periodical measurement of the amount of CHA adsorbed. The adsorption equilibrium was achieved in 4 h.

To obtain the dependence of the amount of CHA adsorbed on the pH, a weighed sample of the CNTs (0.05 g) was brought in contact with 100 mL of a  $1 \cdot 10^{-4}$  M solution of cholic acid. The pH value of CHA solutions was varied in an interval from 2 to 8 by the addition of HCl (or NaOH). After equilibration, the pH of equilibrium solutions was measured. Data for plotting the adsorption isotherm of cholic acid were obtained by contacting the CNT weighed samples (0.05 g) with a  $1 \cdot 10^{-4}$  M solution of CHA, whose volumes were varied. The CHA content in the solutions was determined by the absorbance at  $\lambda = 389$  nm (Specord M-40 spectrophotometer) of a colored complex of cholic acid with concentrated sulfuric acid.<sup>14</sup> The amount of cholic acid adsorbed on the CNT surface was calculated from the difference in concentrations of the initial and equilibrium solutions.

## Results and Discussion

The transmission electron photographs of the synthesized CNTs are shown in Fig. 1. The samples contain

nanotubes with an external diameter of 6–35 nm and an average wall thickness of 2.5 nm. Therefore, the average internal diameter of the cavities is 1–30 nm. The geometric sizes of an CHA molecule ( $0.869 \times 1.453$  nm) are smaller than the internal diameter of the CNTs, which allows cholic acid to penetrate into the nanotube cavities. However, since the CNTs are highly elastic and their length exceeds the diameter by several orders of magnitude, the tubes are curled and balled (see Fig. 1). Kinks of the nanotubes can restrict accessibility of the internal cavities for adsorbate molecules.

The specific CNT surface calculated from the adsorption isotherm of nitrogen (Fig. 2) is  $231 \text{ m}^2 \text{ g}^{-1}$ , the total pore volume is  $0.42 \text{ cm}^3 \text{ g}^{-1}$ , and the micropore volume is  $0.01 \text{ cm}^3 \text{ g}^{-1}$ . The pore size distribution curves of the CNTs show the maximum at 2.8 nm. The electron microscopic data of the diameter distribution of the CNTs suggest that the average internal diameter of the nanotubes is 2.8 nm.

The IR spectrum of the CNTs contains absorption bands at 1626, 1395, 1107, and  $811 \text{ cm}^{-1}$ , which are assigned to stretching and bending vibrations of the C=C, C=O, C—O, and C—C bonds in the oxygen-containing functional groups.<sup>8</sup> The results obtained by X-ray photoelectron spectroscopy confirm oxygen chemisorption on the CNT surface. The total oxygen content in the CNT samples is 11.2% with the following ratio of carbon—oxygen bonds: C—O (6.8%), C=O (3.1%), and O—C=O (4.2%). In the spectrum of 1s electrons of car-

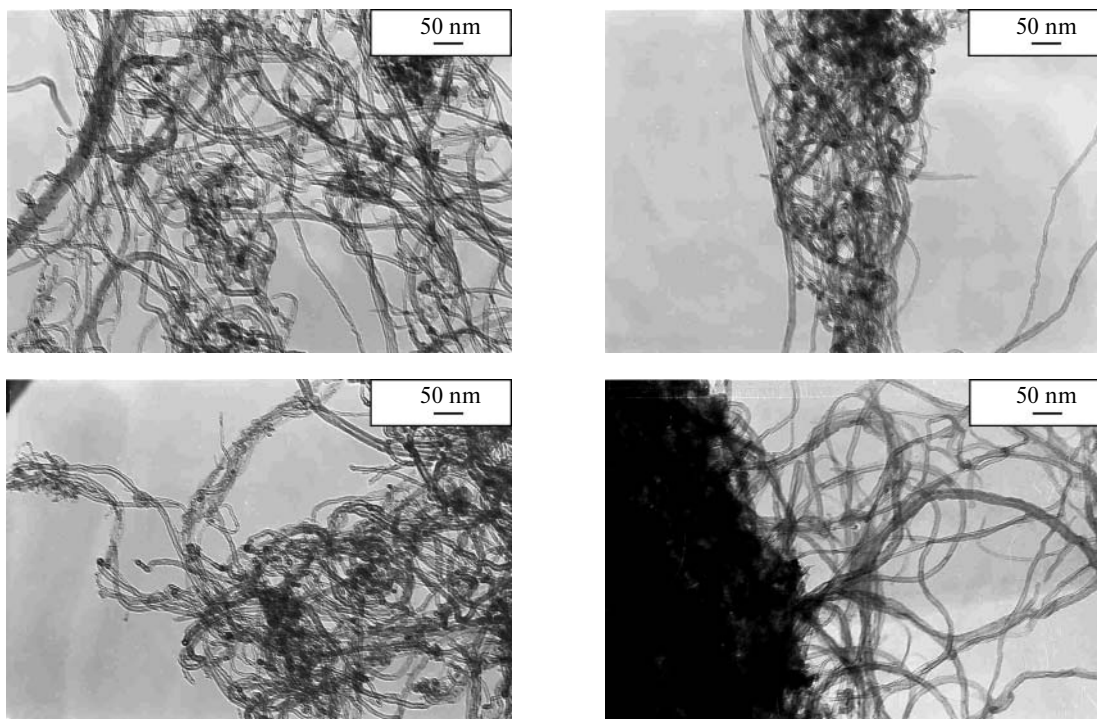
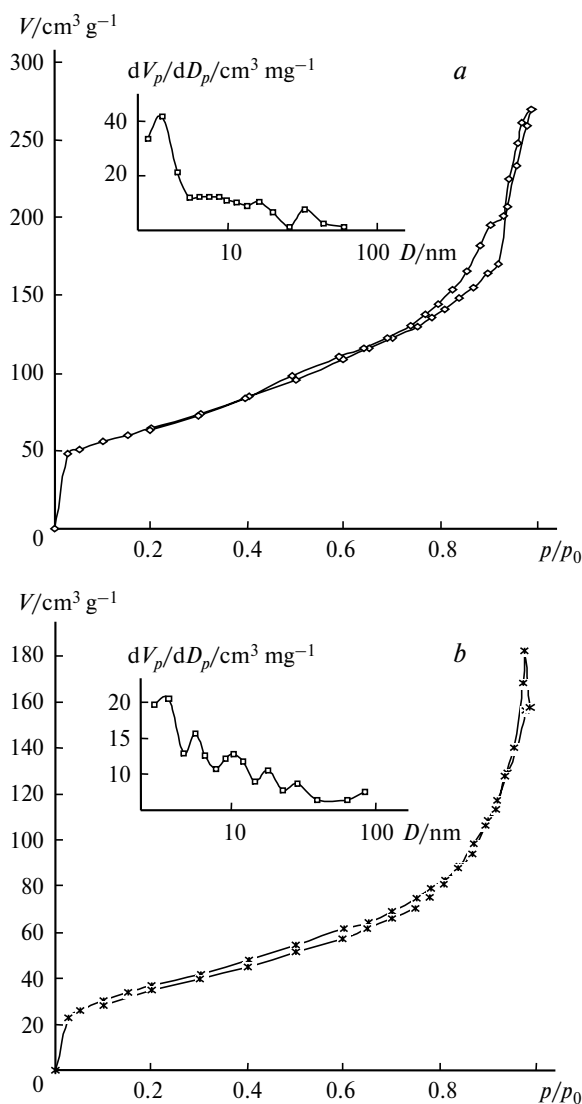


Fig. 1. Transmission electron photographs for different samples of the multiwalled carbon nanotubes.



**Fig. 2.** Adsorption isotherms of nitrogen on the multiwalled carbon nanotubes before (a) and after (b) the adsorption of cholic acid. The pore size distribution curves are shown in insets.

bon (C1s), the maximum of the peak lies at 284.7 eV, and the signal belongs to the skeletal carbon atoms of the CNTs in the state of  $sp^2$ -hybridization.

We have previously<sup>10</sup> found that the Gibbs energy that characterizes the interaction of water with the surface of the CNT samples synthesized by the matrix method is  $542 \text{ J g}^{-1}$ . This value considerably exceeds the Gibbs energy obtained for water adsorption on the majority of carbon sorbents. The reason can lie in high hydrophilicity of sites of primary water adsorption, *viz.*, defects of the CNT surface and oxygen-containing functional groups.

The plot of the amount of cholic acid adsorbed on the surface of the synthesized CNTs *vs.* pH is presented in Fig. 3, *a*. At pH 2–5 the amount of CHA adsorbed is

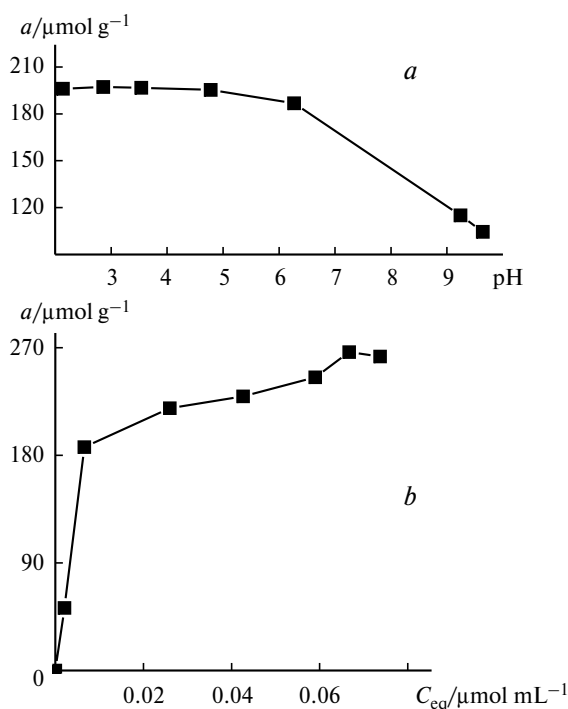


**Fig. 3.** Plots of the amount of cholic acid adsorbed *vs.* pH (a) and the concentration (b) of an equilibrium solution.

$195 \mu\text{mol (g of CNTs)}^{-1}$ , in the neutral region it is slightly smaller, and at pH 9–10 its value decreases by ~40% (down to  $120 \mu\text{mol g}^{-1}$ ). Cholic acid is adsorbed on the CNT surface from weakly acidic solutions in the molecular form. When pH increases, the nanotube surface gains a negative charge due to the dissociation of the carboxyl groups and cholic acid is present in solution predominantly in the form of anions. The mutual repulsion of the negatively charged surface of the nanotubes and cholic acid anions decreases adsorption. However, the amount of CHA adsorbed at pH 8–9 is ~60% of the initial value. This can be taken as evidence for a substantial contribution of hydrophobic interactions to the adsorption of cholic acid.

The adsorption isotherm of CHA on the CNT surface (Fig. 3, *b*) has a shape characteristic of monomolecular adsorption and can be described by the Langmuir equation

$$a = \kappa_1 \kappa_2 C_{\text{eq}} / (1 + \kappa_1 C_{\text{eq}}), \quad (1)$$

where  $C_{\text{eq}}$  is the equilibrium concentration of CHA;  $a$  is the amount of CHA adsorbed;  $\kappa_1$  and  $\kappa_2$  are constants.

The  $\kappa_1$  and  $\kappa_2$  constants calculated from the Langmuir isotherm are equal to  $203 \text{ mL } \mu\text{mol}^{-1}$  and  $274 \mu\text{mol g}^{-1}$ , respectively. Note that despite the low solubility of cholic acid in water, under the experimental conditions, the maximum amount of CHA adsorbed ( $270 \mu\text{mol g}^{-1}$ ) virtually reaches the capacity of the CNTs calculated from

the Langmuir equation ( $274 \mu\text{mol g}^{-1}$ ). The partition coefficient  $K_p$  for CHA adsorption on the CNT surface equals  $1.9 \cdot 10^4 \text{ mL g}^{-1}$ , which is by two orders of magnitude higher than that reported for the sequestrant adsorbents of medical design.<sup>4,5</sup>

After adsorption of cholic acid, the specific CNT surface decreases to  $132 \text{ m}^2 \text{ g}^{-1}$ , the total pore volume decreases to  $0.28 \text{ cm}^3 \text{ g}^{-1}$ , and micropores accessible to nitrogen molecules disappear. Cholic acid adsorption brings about maxima at 2.8, 4.8, 10.1, 10.9, and 11.9 nm in the pore diameter distribution curve for the CNTs. We attributed the maximum at 2.8 nm, as that for the initial nanotubes, to the diameter of their cavities.

The CNT samples<sup>7</sup> contain adsorption sites that show a considerable distribution in energy. The maximum adsorption heat is characteristic of the regions at the boundary between the adjacent CNTs in a plait and the external surface of the carbon nanotubes. Despite energy non-uniformity of the multiwalled CNTs, the adsorption of cholic acid on their surface is described by the Langmuir equation, which indicates that CHA molecules interact with one type of adsorption sites of the CNTs. Taking into account the high adsorption activity of the external CNT surface and the character of a change in CHA adsorption with pH, we can assume that cholic acid is adsorbed on the external surface of the nanotubes and the determining role in the adsorption process belongs to the van der Waals forces.

Adsorption of cholic acid on the multiwalled carbon nanotubes produces an absorption band at  $1404 \text{ cm}^{-1}$  in the IR spectrum, which can be ascribed to CHA adsorbed on the CNT surface. The absence of a noticeable shift of the position of the absorption bands belonging to the

CNTs indicates that the physical adsorption of cholic acid due to nonspecific interactions between the CNT surface and CHA predominates. This conclusion is also confirmed by the TGA data (Fig. 4). The thermal stability of the CNTs is known to depend on the degree of ordering of graphene layers. Multiwalled tubes synthesized by catalytic pyrolysis begin to decompose with a weight loss at  $500^\circ\text{C}$ , which is comparable with the thermal destruction of the CNTs obtained by the matrix method ( $475^\circ\text{C}$ ).<sup>9</sup> For the CNTs synthesized, destruction accompanied by weight loss commences at  $530^\circ\text{C}$  (see Fig. 4). The DTA curve for cholic acid contains thermal effects at 200, 380, 410, and  $530^\circ\text{C}$ , indicating a complicated character of its destruction.

Thermal destruction of the carbon nanotubes containing adsorbed cholic acid resembles that of both CHA and the CNTs. We attribute the decrease in the weight loss in the interval below  $500^\circ\text{C}$  to the destruction of adsorbed cholic acid. Carbon of the nanotubes begins to oxidize with air oxygen at  $530^\circ\text{C}$ , as in the case of the initial CNTs. In the case of chemisorption of cholic acid on the CNT surface, one should expect a substantial shift of the maxima in the DTA curves compared to CHA in the interval from 200 to  $500^\circ\text{C}$ . However, as can be seen from the data in Fig. 4, the temperature intervals of the weight loss of cholic acid in the TGA curves and the position of the thermal effect in the DTA curves differ insignificantly. The results obtained indicate the physical adsorption of CHA on the CNT surface.

Thus, using several physicochemical methods, we found a relationship between the structure and adsorption properties of the multiwalled carbon nanotubes. It was demonstrated that the synthesized CNTs have high parameters of cholic acid adsorption. The adsorption of cholic acid can be mainly related to nonspecific interactions with the surface of the multiwalled carbon nanotubes.

## References

1. A. L. Lehninger, *Principles of Biochemistry*, Worth Publisher, New York, 1982.
2. A. F. Hofmann, *News Physiol. Sci.*, 1999, **14**, 24.
3. S.-D. Clas, *J. Pharm. Sci.*, 1991, **80**, 128.
4. G. M. Benson, C. Haynes, S. Blanchard, and D. Ellis, *J. Pharm. Sci.*, 1993, **82**, 80.
5. L. A. Belyakova, L. N. Besarab, N. V. Roik, D. Yu. Lyashenko, N. N. Vlasova, L. P. Golovkova, and A. A. Chuiko, *J. Colloid Interface Sci.*, 2006, **294**, 11.
6. L. A. Belyakova, A. M. Varvarin, L. N. Besarab, N. N. Vlasova, and L. P. Golovkova, *Zh. Fiz. Khim.*, 2005, **79**, 518 [*Russ. J. Phys. Chem.*, 2005, **79**, 435 (Engl. Transl.)].
7. A. V. Eletskii, *Usp. Fiz. Nauk* [*Progress in Physical Sciences*], 2004, **174**, 1191 (in Russian).

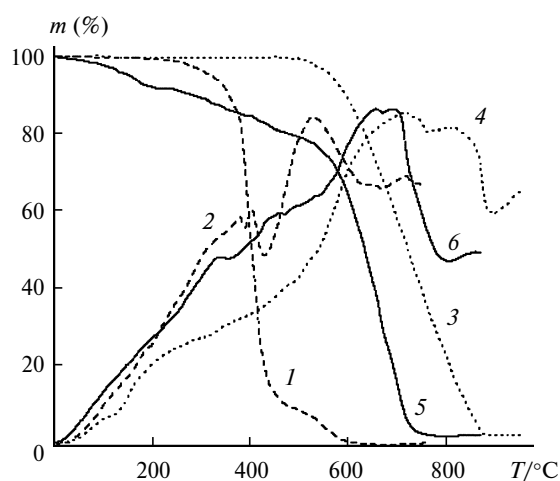


**Fig. 4.** Thermal destruction of cholic acid (1, 2) and the multiwalled carbon nanotubes before (3, 4) and after (5, 6) the adsorption of cholic acid (1, 3, and 5 are TGA data; 2, 4, and 6 are DTA data).

8. S. Ya. Brichka, G. P. Prikhod'ko, A. V. Brichka, and Yu. A. Kislyi, *Neorg. Materialy*, 2004, **40**, 1458 [*Inorg. Materials*, 2004, **40**, 1276 (Engl. Transl.)].
9. S. Ya. Brichka, G. P. Prikhod'ko, Yu. I. Sementsov, A. V. Brichka, G. I. Dovbeshko, and O. P. Paschuk, *Carbon*, 2004, **40**, 2581.
10. V. V. Turov, G. P. Prikhod'ko, S. Ya. Brichka, and M. D. Tsapko, *Zh. Fiz. Khim.*, 2006, **80**, 1 [*Russ. J. Phys. Chem.*, 2006, **80**, 591 (Engl. Transl.)].
11. A. V. Melezhik, Yu. I. Sementsov, and V. V. Yanchenko, *Zh. Prikl. Khim.*, 2005, **78**, 938 [*Russ. J. Appl. Chem.*, 2005, **78** (Engl. Transl.)].
12. E. P. Barret, L. G. Joyner, and P. P. Halenda, *J. Am. Chem. Soc.*, 1951, **73**, 373.
13. R. J. P. Corriu, R. Perz, and C. Reye, *Tetrahedron*, 1983, **39**, 999.
14. R. M. C. Dawson, D. C. Elliot, W. H. Elliot, and K. M. Jones, *Data for Biochemical Research*, Clarendon, Oxford, 1986.

Received June 19, 2006;  
in revised form September 12, 2006